ChemComm

Accepted Manuscript

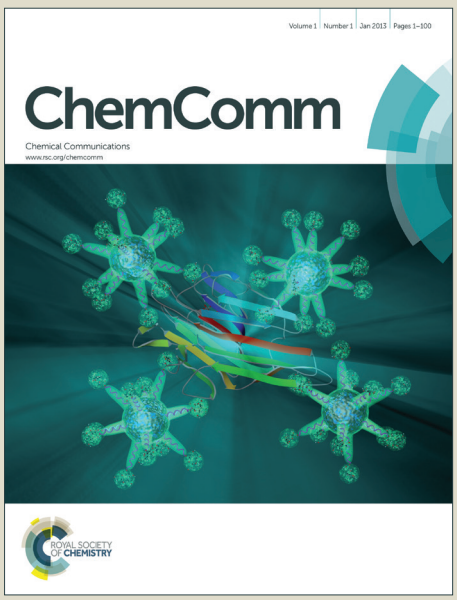

ROYAL SOCIETY OF CHEMISTRY

www.rsc.org/chemcomm

ARTICLE TYPE www. rsc.org/xxxxxx | XXXXXXXX

Modelling flow-induced crystallisation in polymers

Richard S. Graham

Received Xth XXXXXXXXXX 20XX, Accepted Xth XXXXXXXXX 20XX
First published on the web Xth XXXXXXXXXX 200X
DOI: 10.1039/b000000x

Flow profoundly influences the crystallisation kinetics and morphology of polymeric materials. By distorting the configuration of polymer chains, flow breaks down the kinetic barriers to crystallisation and directs the resulting crystallisation. This flow-induced crystallisation (FIC) in polymers is a fascinating, externally driven, non-equilibrium phase transition, which is controlled by kinetics. Furthermore, the effect is of central importance to the polymer industry as crystallisation determines virtually all of the useful properties of semi-crystalline polymer products. However, simulating flow-induced crystallisation in polymers is notoriously difficult due to the very wide spread of length and timescales, especially as the most pronounced flow-induced effects occur for long chains at low undercooling. In this article I will discuss multiscale modelling techniques for polymer FIC. In particular, I will review recent attempts to connect modelling approaches across different levels of coarse-graining. This has the ultimate aim of passing insight from the most detailed simulation techniques to more tractable approaches intended to model polymer processing. I will discuss the exciting prospects for future work in this area.

1 Introduction

Flow-induced crystallisation (FIC) is one of the outstanding unsolved problems in polymer science. The problem contains significant fundamental science, having at its heart the dynamics of a non-equilibrium phase transition. Simultaneously, understanding polymer FIC is of great practical importance due to its potentially transformative impact on the polymer industry. However, the field presents some formidable theoretical difficulties due to the wide separation of length and timescales. Nevertheless, recent theoretical work has begun to illuminate a pathway to a quantitative understanding of polymer FIC from molecular principles.

The basic experimental phenomena for FIC in polymers were observed nearly 50 years ago[1]. It is now well-established that polymer crystallisation is profoundly influenced by flow[2]. Flow drastically enhances the rate at which polymers crystallise and has a profound effect on their morphology. Flow distorts the configuration of polymer chains and, it is believed, this distortion breaks down the kinetic barriers to crystallisation and directs the resulting morphology.

Polymer crystallisation is very susceptible to flow for the following reasons. Firstly, polymer crystallisation begins with nucleation, which is extremely rare on a molecular scale. Small crystallites are unstable due to the free energy cost of their interface with the liquid. This creates a free energy barrier to nucleation, which the system must diffuse over via a thermally activated process. The nucleation rate depends exponentially on the barrier height. Thus any change in the nucleation barrier will drastically alter the nucleation rate and nucleus density. Secondly, due to their long chain nature, polymer crystallise into a composite structure of ordered crystalline regions interspersed with amorphous regions, in which the chains are randomly arranged. These structures do not correspond to the equilibrium state, meaning that the crystallisation is incomplete and is kinetically selected. Hence, the flow conditions experienced by a polymer fluid, prior to and during crystallisation, can determine its morphology.

FIC is ubiquitous in industrial polymer processing Fig 1 shows polymer crystallisation during a prototype industrial flow[3,4]. The darker regions are developed crystals and these grow preferentially in regions where the flow field is most intense. Thus control of flow conditions offers the tantalising potential to control the crystallisation and morphology of semi-crystalline polymeric materials. This is of great interest to the polymer industry as the crystal properties strongly influence strength, toughness, permeability, surface texture, transparency, capacity to be recycled and almost any other property of practical interest. This offers the possibility of molecular design of polymer products. However, achieving this requires a molecular understanding of polymer FIC.

Accurate modelling of polymer FIC involves some of the most challenging problems in polymer science. Strong chemical bonds force connected atoms to move co-operatively, whereas unbonded atoms interact through weak van der Waals forces. This leads to a huge separation of both time and length-scales. Under flow polymers crystallise into elaborate hierar-

School of Mathematical Sciences, University of Nottingham, Nottingham NG7 2RD, United Kingdom. Fax:+44 115 951 4951; Tel: +44 115 951 3850; E-mail: Richard.Graham@nottingham.ac.uk

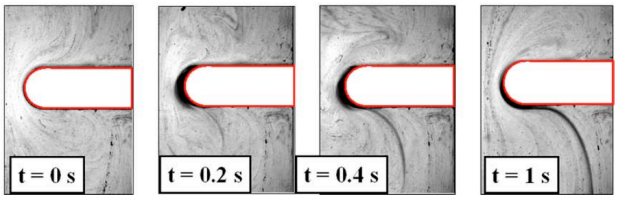

Fig. 1 Bright field observation of polymer crystallisation during complex flow of a high-density polyethylene resin. The flow direction is top to bottom, t indicates the time since inception of flow, the flow rate is 1cm^3/sec and the cross sectional area at the entrance is 1cm^2. Reprinted with permission from Scelsi *et al.*[3]. Copyright 2009, The Society of Rheology.

chical structures (see for example the sketch in fig 2). In these structures the monomer repeat units of length ~ 0.1 nm self assemble into crystal structures that can be $\gtrsim 100$nm. Even more problematic is the separation of timescales. Monomer relaxation times are $\sim 10^{-9}$sec whereas the time to nucleate and self-order into a fully developed structure be several hours ($\sim 10^4$sec). These issues are particularly prominent as the regimes of high molecular weight chains and low undercooling, which are the most challenging region to simulate, are precisely where the most pronounced flow-induced effects occur. Indeed, recent experiments show that insight into low undercooling is essential to both a fundamental and practical understanding of polymer FIC[5–7]. There are two fundamentally different contributions to these computational difficulties. Firstly, nucleation is a rare event. That is, nucleation is characterised by very frequent attempts to form a stable nucleus, with very occasional successes. A successful nucleation event is, itself, fast, but requires long simulation times because it occurs so rarely. Secondly, because of their length, long polymer chains carry significant monomer drag. Thus their diffusion dynamics are extremely sluggish. For example, for concentrated long chains[8], the terminal relaxation time scales with molecular weight as $M_w^{3.4}$. Therefore, any process that relies on global relaxation of the polymer chains will be slow, not due to its rareness, but the sluggish dynamics that underlie it. These two types of slow process present very different computational challenges and require tailored solutions.

Despite the great variation in the chemistry between crystallisable polymers, there is a high-degree of universality in their crystallisation dynamics, suggesting the possibility a powerful universal model, applicable to many systems. Such progress requires several levels of modelling techniques to address the length and timescale difficulties. The individual levels of modelling need to be tightly integrated to enable insight gained from the most detailed approaches to be inherited by the more tractable models. Such modelling would improve our fundamental understanding of polymer FIC and produce tractable computational tools for practical applications.

In this review I describe recent experimental and theoretical progress in sections 2 and 3, respectively. I discuss potential future directions in section 5, while also highlighting important open questions and outstanding modelling issues. Section 6 contains summary and conclusions.

2 Experiments

2.1 Enhanced nucleation

Well-controlled flow experiments, mostly under shear, confirm the strong effect of flow on crystallisation[2]. Crystallisation during or following flow has been monitored with a range of time resolved techniques, such as small angle x-ray scattering[9], birefringence[10,11] and linear oscillatory shear[12,13]. These measurements show that the crystallisation rate progressively increases with deformation rate[14] and that the number of nuclei increases increasing flow time, t_f[15]. The combined effect of flow rate and time can be summarised by the macroscopically applied work, w,

$$w = \int_0^{t_f} \boldsymbol{\sigma}(t) : \mathbf{D}(t) \mathrm{d}t, \qquad (1)$$

where $\boldsymbol{\sigma}$ and $\mathbf{D}$ are the stress and deformation rate tensors, respectively. The nucleation density, for a given material and temperature, is a universal function of w, covering both shear and extensional flow[16]. There are some exceptions to this empirical rule. For example, the influence of t_f on the crystallisation kinetics saturates for long shearing times[10]. Furthermore, there is a critical shear rate below which the crystallisation kinetics are identical to quiescent conditions[12]. This critical shear rate can be correlated the material's relaxation time.

In many of the above experiments, the increased nucleation was indirectly inferred through a decrease in the crystallisation half time. However, optical observations allow a direct determination of the nucleation rate or density essentially by counting nuclei. For example, Stadlbauer *et al*[16] quantified the total nucleation resulting from a wide range of flow pulses and Pantani and co workers directly measured the nucleation rate during steady continuous shear flow,[17,18]. These experiments separate the influence of nucleation and crystal growth and the resulting nucleation data provide a fundamental quantity, against which models can be quantitatively tested.

A consistent picture of the influence of temperature, emerges from many of the above studies: the sensitivity of the crystallisation kinetics to flow increases with increased temperature. At low-undercooling the nucleation is extremely tenuous and it is the rareness of the nucleation process makes it more susceptible to flow. I will describe in section 4.1.3 a molecular explanation for this effect.

2.2 Shish kebab formation

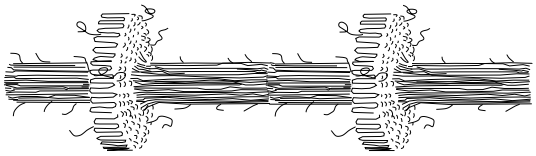

Fig. 2 A schematic diagram of the shish kebab morphology, as observed experimentally [1,5,11,19].

At moderate shear rates the flow-induced nuclei are point-like and grow into a spherical crystal structure. However, at higher flow rates a striking transition to elongated row-like nuclei occurs [1,5,6,19]. Around these long slender nuclei, subsequently grow plate-like lamellae of folded chains. This distinctive morphology, known as the shish-kebab (fig 2), improves mechanical properties [20] and reduces permeability [21].

Flow enhanced nucleation and particularly shish kebab formation are strongly influenced by the high molecular weight tail of a melt's molecular weight distribution [6,9,11]. This high molecular weight tail contains the longest chains in the melt and, due to their long relaxation times, these chains are most readily stretched under flow. Indeed the composition of the high molecular weight tail can be varied by blending a small amount of long chains into a shorter matrix polymer. FIC experiments on such blends have shown that the long chain concentration controls the number density and thickness of shish nuclei [10,11]. Furthermore, several studies have reported drastic changes in shish formation when the concentration exceeds the overlap concentration for the long chains [9,11]. Carefully controlled neutron scattering experiments have revealed the relative concentration of long chains in the shish structure [5]. These experiments show that, despite being more readily stretched, long chains are not more abundant in shish than in the melt as a whole. This suggests that the long chains catalyse the shish formation and are able to recruit chains of all lengths into the shish. Li and coworkers [22–24] have studied the effect of extensional flow on the crystal morphology. By examining different extensional strains [23], they found a correlation between the morphology and the material's stress response to the imposed strain. Further measurements also demonstrated that, not only do long chains promote nucleation by changing the melt free energy, they also prevent rupture through their influence on the macroscopic stress, which enables larger strains to be achieved [24].

Similarly to enhanced nucleation, the macroscopic work, (equation (1)), also strongly influences the formation of shish kebabs. Mykhaylyk *et al.* [6] demonstrated that a single critical value of the applied work determines the onset conditions for oriented crystallisation over a wide range of flow conditions. Further common effects with enhanced nucleation are seen in the temperature dependence of shish kebab formation. Here the anisotropy increases with increasing temperature [25].

There is a growing consensus that shish kebabs nucleate via precursors that comprise of metastable, elongated domains with an intermediate degree of order. By studying a specially synthesised linear high density polyethylene with a bimodal molecular weight distribution, Balzano *et al.* [26,27] have shown that four different structure can be formed: non-crystalline precursors, shish, kebabs and quiescent crystals. These structures have remarkably widely separated formation temperatures given by 142°C, 139°C, 132°C and 124°C, respectively. Furthermore, their experiments on isotactic polypropylene [28] indicate that only the non-crystalline precursors can form during flow itself, with the crystalline structures appearing rapidly but only after flow has ceased. This is a very different scenario to enhanced point-like nucleation under flow, where Pantani and co-workers [17,18] observed spherulite growth during steady shear. Work by Azzurri, Alfonso and coworkers [29–31] has established the dependence of the precursor lifetime on temperature, molecular weight and shear conditions. They have studied polydisperse iPP [31] and isotactic poly(1-butene) [29] and monodisperse isotactic polystyrene (iPS) [30]. They demonstrated that the dissolution timescale depends upon shear rate, suggesting that shear changes the precursor morphology, while the activation energy is independent of flow rate and molecular weight, indicating that the rate-limiting step of the dissolution involves relatively short segments of chain and is independent of shear history. Studies by Kanaya and co workers [7,32–35], have provided further details of the shish processor. Their measurements on iPP, confirm that an oriented precursor can be formed above the melting temperature for folded chain crystals and that this precursor is denser than the melt but not necessarily crystalline [35]. Their measurements on iPS have revealed significant new details about the nature of the precursor. Large string-like precursors precede the formation of shish crystals. These structures can be imaged directly by polarised optical microscopy (POM) and are on the μm scale [32]. The precursors form and persist significantly above the melting temperature for folded chain crystals [32,33] and, when cooled, are able to nucleate shish kebabs. The structure of the precursor is not fully established. It may be an oriented gel-like structure, stabilised by extended chain crystals or may have a liquid-crystal structure, in which rigid chain segments in a helix configuration function as mesogens. Very recent measurements [7] investigating the inner structure of the precursor, show it has very low crystallinity ($\sim$ .15%) with a small fraction of extended crystals, of similar length to shish crystals. Hashimoto and co workers [36,37] have studied the effect of flow-induced liquid-liquid phase-separation in a polymer solution, on the very early stages of shish formation. They proposed a sequence of steps by which phase-separated domains that are rich in stretched chains ultimately

lead to shish kebab formation. The authors also argue that this phase separation will occur in bimodal and polydisperse melts whenever there is a sufficiently wide separation of timescales. The full nature and formation mechanisms of the shish kebab structure remains under considerable debate.

2.3 Polydispersity and model materials

The overwhelming majority of FIC experiments are performed on polydisperse polymers. That is, melts with a broad distribution of chain lengths. For such melts, dilute long chains that are deep into high-molecular weight tail will contribute strongly to FIC, as these chains deform the most under flow. Thus measurements from polydisperse materials contain simultaneous contributions from many different molecular lengths, each executing widely differing dynamics. This makes direct interpretation of the results very problematic. Unfortunately, it is extremely difficult to synthesise monodisperse crystallisable polymers, even on the small scale required for well-controlled lab experiments[9] (of order a few grammes). A small number of studies have involved blends whose fractions are individually narrowly distributed[6,9,30,38,39]. Such model materials enable a much more precise definition of key molecular quantities such as the long concentration, overlap concentration and molecular relaxation times. For example, one such study[6] established that shish kebab formation can only occur if the deformation rate exceeds the molecular relaxation time associated with chain stretching.

3 Modelling

As described in section 1, polymer FIC inherently involves a very large separation of length and timescales. Multiscale modelling is an essential tool in addressing these issues and modelling techniques have been developed at a range of levels. Fig 3 summarises the currently employed techniques, in order of detail and computational cost. However, when trading a less detailed description for improved computational speed, ambiguous coarse-graining decisions and new undetermined model parameters are virtually inevitable. Thus, a key ongoing challenge is to interface modelling approaches on different levels. This would allow detailed models to motivate and justify assumptions made in more tractable approaches.

Of the two computational challenges discussed in section 1, coarse-graining is most effective at tackling the issue of slow diffusion. This is because, coarse-graining essentially integrates out the faster degrees of freedom, allowing longer timesteps to be taken. This still leaves the difficulties of simulating rare events. However, when working with more coarse-grained models it is often easier to apply algorithmic tools that deal with rare events, as I will demonstrate below.

3.1 Classical nucleation theory

Classical nucleation theory provides an analytic framework to describe basic nucleation phenomena[41,42]. The nucleation problem comprises of a nucleation barrier $F(n)$ (see fig 4), where F is the free energy of a nucleus of n particles. Here F is expressed in units of k_BT and $\Delta F(n) = F(n) - F(0)$. The nucleation barrier can be calculated if σ, the free energy of the melt-crystal interface, and ΔG, the Gibbs free energy difference between the crystal and melt phases, are both known. In principle, ΔG can be calculated from the degree of undercooling. However, this requires an accurate knowledge of the properties of the phase into which nucleation occurs. This is not always straightforward to obtain for polymers, as the nucleated phase may not be the final crystal phase[43]. The interfacial energy σ is even harder to obtain and is often treated as a parameter to be fitted to experimental data.

The local diffusion rate $D(n)$ changes with nucleus size n as the nucleus surface area increases with size. In order to nucleate, the system must diffuse over the barrier peak and continue a sufficient distance down the other side that re-crossing is negligibly improbable. Briefly, Kramers' method[41] solves the diffusion equation with an absorbing boundary condition placed beyond the barrier peak and a constant input flux of new nuclei at the barrier base. The crossing rate can be inferred from the steady state number of nuclei in the system.

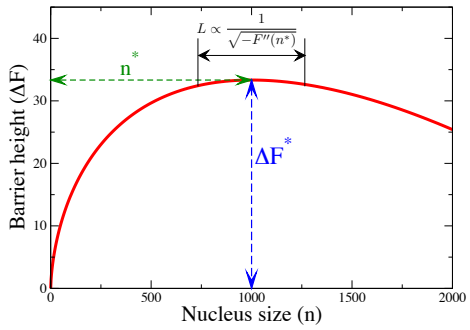

Fig. 4 A 1D nucleation barrier, illustrating the quantities n^* (critical nucleus size), ΔF^* (barrier height) and L (plateau width), which make important contributions to the nucleation rate.

Kramers' problem can be solved for an arbitrary barrier $F(n)$, but to simplify the resulting expression I have made the following assumptions, which are typically true for nucleation: the barrier peak is $\Delta F^* \gg k_BT$; the barrier is steep at the base; the barrier peak is a smooth maximum; and the diffusion kinetics do not change significantly along the barrier peak. Although, the problem can be solved for discrete or continuous n, I use here the continuous representation for mathematical clarity. More detailed discrete treatments that relaxes some of the above assumptions are possible[44].

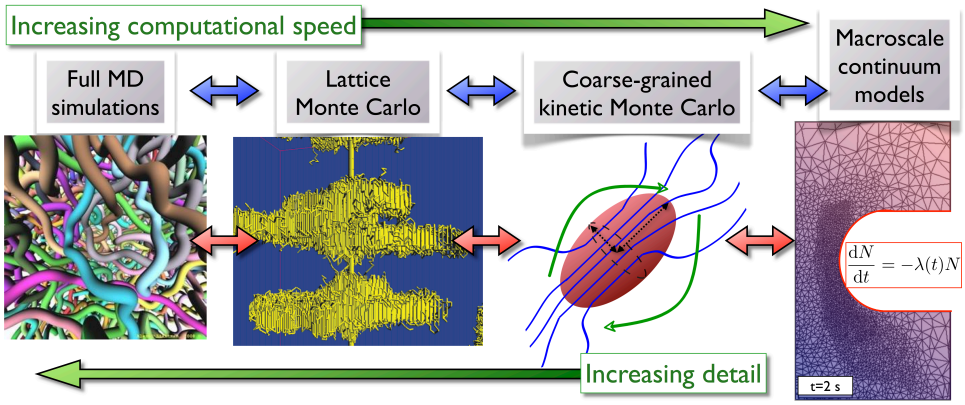

Fig. 3 Progressively increasing levels of coarse-graining in modelling polymer crystallisation. MD figure courtesy of Prof. A Likhtman and Lattice MC figure courtesy of Prof W Hu, reprinted with permission from Hu *et al.*[40], copyright 2002 American Chemical Society.

Employing Kramers' method leads to an analytic expression for the nucleation rate $\dot{N}$,

$$\dot{N} = \frac{1}{\sqrt{2\pi}} \left[\frac{1}{Z} \exp(-\Delta F^*) \right] \left[D(n^*) \sqrt{-F''(n^*)} \right], \quad (2)$$

where Z is the barrier partition function, considering only the base up to the peak $Z = \int_0^{n*} \exp(-F(n)) \mathrm{d}n$. For a sufficiently steep initial barrier $Z \approx \frac{1}{F'(0)}$. This nucleation rate expression can be understood at a scaling level as follows. The first square bracket is the equilibrium occupancy probability at the barrier peak (i.e. the fraction of time that the system spends around the barrier peak). Having reached the peak, in order to successfully cross, nuclei must diffuse along the plateau, sufficiently far that the chance of returning to the barrier base is vanishingly small. Hence the plateau is defined as the region around n^* over which the barrier remains within unity of F^* (see fig 4). Thus the plateau length L scales as $1/\sqrt{-F''(n^*)}$. Therefore the term in the second square bracket corresponds to the flux across the plateau at the barrier peak.*

Kramers' method can be generalised to $N-$dimensional barriers, leading to a comparable expression for the crossing rate[41]. However, this is limited to a modest number of dimensions because locating the barrier peak in high-dimensions is usually prohibitively expensive. Thus application of classical nucleation theory is limited to low-dimensions, in contrast to the very high number of degrees of freedom in molecular system. Motivated by classical nucleation theory, I will discuss a method to project high-dimensional nucleation problems on to lower dimensional systems in section 4.1.2.

In summary, classical nucleation theory enables calculation of the nucleation rate from the barrier shape, $F(n)$, and the diffusion kinetics, $D(n)$. For conditions that are typical of nucleation, the important barrer properties are the height of the peak, $F(n^*)$, the initial gradient, $F'(1)$, and the plateau length, characterised by $F''(n^*)$. Other features of the barrier contribute only weakly to the crossing rate. Similarly, only the diffusion kinetics at the barrier peak, $D(n^*)$, contribute significantly to the crossing rate. These ideas will form the basis of a fast algorithm for simulating nucleation in section 4.1.1.

3.2 Macroscale Continuum models

A key aim of modelling polymer FIC is to provide tools to model polymer processing. Modelling polymer processing invariably involves computations in complex flow geometries (for example, see fig 1). Tractable modelling of FIC in these complex flow geometries requires equations that are free of stochastic terms. These macroscale continuum models typically use ordinary differential equations to describe the crystallisation kinetics under flow. These are usually formulated using the Schneider/Kolmogorov rate equations[45,46], which compute the crystal evolution, provided nucleation and growth rates are known functions of time. These models provide many details of the crystallisation, including spherulite density, radius, surface area and volume. They are also computationally inexpensive and so can be used in finite element calculations in complex flow geometries[47].

A significant disadvantage is that this level of modelling cannot predict how the nucleation rate depends upon chain deformation under flow, Macroscale models require, instead, this to be an input assumption. Such models typically assume an empirical dependence of the nucleation rate on the flow conditions[15], the stress tensor[48], or the chain stretch[49,50]. Often these functional forms are chosen empirically to best describe available data. This step severs the link with molecular modelling. Furthermore, changes with molecular weight

* The crossing flux scales as $1/L$ rather than $1/L^2$, which might be anticipated for a diffusion problem. This is because visits to the barrier peak (from the first term) specify a constant probability density at the boundary of the plateau region rather than a zero flux boundary condition which gives $1/L^2$ scaling.

distribution and temperature cannot be dealt with in a systematic way. Thus the expressions used for nucleation in such models usually contain uncontrolled parameters and require extensive characterisation against experiments. This characterisation must be repeated for each new resin, as changes in the molecular weight distribution between batches is common. These difficulties proliferate when these models are generalised to the nucleation and formation of shish kebabs.

A notable approach at this level of modelling has recently been developed by Howard and Milner[51]. They used a 2D version of classical nucleation theory, combined with a "cylindrical cap" nucleus model to describe isotactic polypropylene. A key element is that the unknown interfacial energies are not just extracted from experimental data, but also confirmed against all-atom lattice dynamics simulations[52]. Consequently, their approach deals with temperature in greater detail than comparable models. This work highlights the potential of multiscale modelling to exploit the strengths and overcome the weaknesses of each level of modelling. Although, the approach currently only pertains to quiescent nucleation, the authors also discuss the possibility of extension to FIC.

3.3 Molecular dynamics

At the highest level of detail, molecular dynamics (MD) simulations provide a rigorous approach to crystallisation by resolving the motion of individual monomers. Previous work has established suitable united-atom force fields for polyethylene[53–57] and polypropylene[58]. MD potentially provides a wealth of detailed information on polymer crystallisation and its dependence on molecular weight, temperature and flow. I provide a brief review here. A more detailed review, focussing primarily on MD, has recently been made by Yamamoto[59].

Many studies have focussed on crystal growth, providing a detailed molecular picture of how it depends on molecular weight and temperature. Simulations have validated and parameterised a model that decomposes the growth rate into contributions from secondary nucleation at the growth front and molecular diffusion of chain segments[60]. Simulations have also elucidated details of tapering at the growth front, lamella thickening and chain folding at the lamella surface[61].

Some MD studies have observed primary nucleation in polymers[53,55–57]. Yamamoto analysed the supercooled melt structure during homogeneous nucleation, observing changes in the radius of gyration and persistence length[55]. Rutledge and coworkers[53,62] observed nucleation during a uniaxial extension flow. They used flow rates with Weissenberg numbers of $Wi \gtrsim 2$ †, which is comparable to processing conditions and well-controlled experiments. These simulations demonstrated that flow enhances nucleation, if the strain is sufficient. In these simulations, no crystallisation was observed during flow itself and crystallisation was delayed until cessation flow, after which it proceeded at a much enhanced rate. This is in accord with experiments of Balzano *et al*[28]. Further simulations on the same system[53] revealed how temperature affects the balance of the nucleation and chain relaxation rates as they compete to determine the crystallisation kinetics.

MD has the key limitation that computational expense restricts the accessible timescales to typically $\sim$ 10ns. Computational cost also restricts the chain length due to the limited simulation box size. Therefore nucleation in MD simulations can only be observed for short chains at high undercooling, where the simulation temperature is set far below the crystallisation temperature. Lowering the temperature increases the thermodynamic driving force for crystallisation, which drastically increases the nucleation rate to within the simulation timescale. However, this fast nucleation at high-undercooling is likely to have a different mechanism to the low undercooling that is typical in polymer processing. For example, Yamamoto[55] observed an unexpectedly steep increase in the persistence length at large undercooling. This suggests that, at low undercooling a strong increase in chain stiffness, may assist nucleation. Furthermore, experiments show that insight into both low undercooling and long chains is essential to both a fundamental and practical understanding of FIC[5,6], as the most pronounced flow-induced effects occur in these regimes.

MD can deliver highly resolved molecular detail of the crystallisation process, with very few modelling assumptions. However, it suffers from strong lengthscale and timescale limitations. Thus further work is needed, building on the above MD are studies, to address issues with simulating rate events, to quantify the nucleation rate and to build connections with more coarse-grained simulations. Very recent MD studies[57] have begun to address these issues and to extract unknown parameters for classical nucleation theory from molecular simulation. I will discuss this recent progress in section 4.2.

3.4 Lattice Monte Carlo

Lattice Monte Carlo (MC) methods[40,63–65], restrict polymer chains to a regular lattice and model the dynamics as discrete hops between lattice sites. This significantly reduces the computational cost of evaluating the system's potential energy and hugely increases the simulation timestep. This allows larger chains to be simulated for longer timescales, compared to MD. The potential energy has contributions from the number of parallel (nonbonded) bonds on neighbouring sites, the number of chain-solvent contacts and the number of kinks along the each chain. The dynamics are described by a micro-relaxation model. Polymers move either by local jumps, involving single monomers or by sliding moves, involving longer chain segments. The sliding moves greatly increases the sampling rate

† The Weissenberg number is defined as Wi = (flow rate) $\times$ (material relaxation time), giving a dimensionless comparison of flow against relaxation.

and mimic the real dynamics of polymers in dense systems.

Despite the gains in computational speed, the rare event issue still means that nucleation is difficult to simulate, especially at low undercooling. However, using a combination of biased sampling, multi-histogram techniques and parallel tempering[66], Hu *et al.*(2003)[63] determined the free-energy barrier for nucleation of a single-homopolymer chain. They also explored the strong dependence of the barrier on molecular weight, as they could simulate chains of several hundred repeat units. The application of a similar simulation algorithm to thin films of short polyethylene[65] chains observed primary nucleation directly. Nucleation occurred during the simulation timescale because of a relatively deep quench and because nucleation is faster at the film free surface than in the bulk.

Hu *et al.*(2002)[40] have used chain alignment to enhance the primary nucleation rate. They simulated a system of free chains with a single, fully aligned chain spanning the simulation box. Simulations were performed below the melting temperature but above the temperature at which homogeneous nucleation was accessible on simulation timescales. The free chains rapidly formed rows of crystal nuclei along the stretched chain. These nuclei then grew into plate-like lamellae (see fig 3), essential reproducing the experimentally observed shish-kebabmorphology (fig 2). These simulations confirm that even a single aligned chain can both accelerate crystal nucleation and initiate the formation of shish kebabs.

Recently, Hu and co-workers[67] imposed a homogenous stretch to a bulk melt and then used dynamic Monte Carlo to observe strain-induced nucleation. These simulations could be run close to the melting point. Beyond a critical strain, the nucleus morphology shifted from isotropically-oriented chain-folded nuclei to aligned fringed-micelle nuclei (similar to fig 5). These authors also extended this work to strain induced nucleation in random co-polymers[68]. The non-crystalline co-monomers mimic the effect of sequence defects that are found in industrial polymers. Increasing co-monomer content increases the onset strain for crystallisation, which could be explained by a thermodynamic model.

Although lattice MC simulations lead to significant gains in accessible chain length and timescale compared to MD, they require coarse-graining assumptions. The algorithm must postulate which moves are dynamically the most relevant. Numerous types of moves can be imagined and the relative frequency of attempts of these moves must also be assumed. Also the course-graining of the molecular potential leads to new unknown parameters, such as the energy cost of separating a pair of parallel bonds. Finally, it is not always clear how the predictions are affected by confining chains to a discrete lattice. Thus there is a need to compare results with MD simulations, where the windows of plausible time and length scales for the two techniques overlap, in order to provide guidance on the assumptions inherent to the lattice MC method.

3.5 Coarse-grained kinetic Monte Carlo

3.5.1 Model outline I recently developed a highly coarse-grained simulation algorithm for polymer nucleation, the Graham and Olmsted (GO) model[69,70]. The model aims to bridge between detailed simulations and macroscale continuum models; to utilise detailed rheological models that have proven successful in predicting the flow dynamics of non-crystalline polymers[71,72]; and to be suitable for comparison with experimental data. The model is also simple enough to allow the use of rare event simulation techniques and to enable a projection onto a low-dimensional model. The model uses a kinetic Monte Carlo algorithm with an adaptive time-step[73]. This algorithm has previously been applied to highly coarse-grained simulation of crystal growth in polymers[74,75]. However, it is also well suited to nucleation as, for small nuclei where progress is slow, large timesteps are automatically taken.

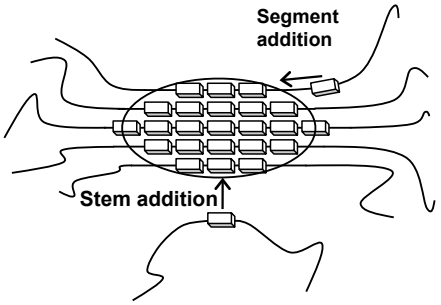

Fig. 5 A diagram of the nucleus description used in the GO model[69,70] . Crystallised monomers are arranged in stems, with amorphous chains protruding from the surface. The whole structure can be rotated by the flow A 2-D cross section of the 3-D ellipsoid polymer nucleus with an illustration of the two possible moves which add one Kuhn step to the nucleus.

The simulation takes a minimal nucleus description that is still able to model both enhanced nucleation and shish formation (see fig 5). The nucleus comprises N_T crystallised monomers, arranged in N_s stems, with each stem formed from a single chain. The number of monomers in each stem, is tracked during the simulation, with the arrangement of the monomers within the crystal not being resolved. The nucleus is assumed to be spheroidal, which allows both the volume and surface area to be computed from N_T and N_s. The nucleus free energy consists of a bulk free-energy reduction due to crystallisation, proportional to the nucleus volume, and a free-energy penalty proportional to the spheroid surface area. Nuclei evolve by addition and removal of individual particles and there are two ways to add a monomer: addition of a monomer onto an existing stem or addition of a new stem. The rate of these individual steps is calculated from the free-energy change resulting from the step. It is here that the effect of flow is implemented. The deformation of the surrounding chains

under flow is computed using a separate rheological model, known as the GLaMM model[71]. From the configurations of the surrounding amorphous chains, provided by the GLaMM model, the entropy loss due to stretching can be calculated. This entropy loss is deducted from the bulk term in the free energy, creating a stronger thermodynamic driving force for crystallisation. The degree of polymer deformation depends on position along the chain contour, with monomers close to the chain centre being most deformed, while those close to the chain ends remain undeformed. Thus there is a wide spectrum of differently stretched chains sections, leading to a corresponding spread in attachment rates. If the polymer melt also contains a spread of molecular weights, then the range of attachment rates will be wider still.

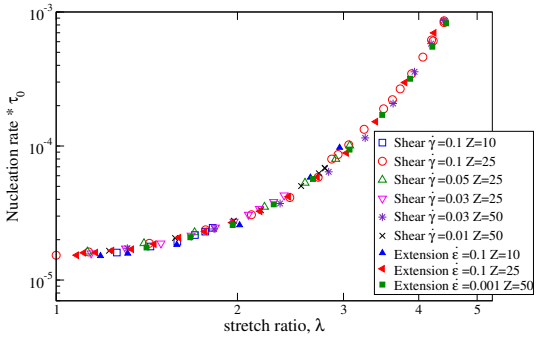

Fig. 6 A master curve of nucleation rate against stretch ratio for a range of molecular weights, flow rates and flow geometries. Here Z is the dimensionless molecular weight expressed in terms of the molecular weight between entanglements[8].

3.5.2 Results A number of key results were produced by direct simulation of the GO model. Simulations predict the formation of highly elongated nuclei, at higher shear rates. Essentially, the shish nuclei are seeded by a small number of stretched chain segment and lengthening of the nucleus is driven by these stretched chains crystallising by zipping-up along the chain. In the simulations, shish nuclei are produced more readily in bimodal blends than in monodisperse melts and the anisotropy is increased by decreased undercooling, both of which are seen experimentally.

A second key result is that nucleation during a transient flow is quasi-static. That is, the nucleation rate depends only on the instantaneous barrier, not its prior history. Therefore the instantaneous nucleation rate can be found by solving the much simpler static problem obtained by holding the amorphous chain configurations fixed at that corresponding to time of interest. This quasi-static result arises essentially because the evolution of the nucleation barrier is slow compared to the time taken for a successful nucleation event to traverse from the barrier base to beyond the barrier peak.

The quasi-static result can be further extend to show that the simulated nucleation rates have a universal dependence on the chain-stretch ratio (defined as the polymer length normalised by its quiescent value), independent of flow rate, molecular weight and flow geometry. Fig 6 shows an example master curve, for a fixed degree of undercooling. It should be noted that the shape of the master curve depends upon the quiescent free energy landscape. In particular as the quiescent barrier height increases so does the sensitivity to flow. As the barrier height increases with temperature, the model correctly predicts that flow sensitivity increases with temperature, as in experiments[12,18]. The later two results justify some of the tacit assumptions in macroscale continuum models. Furthermore, the nucleation rate against stretch master curve provides the molecularly motivated expression for the nucleation rate that is missing from macroscale continuum models.

A successful comparison of the GO model with nucleation rate measurements from a flowing isotactic polypropylene melt under has also been made[70]. This comparison has recently been extended[76] using the enhanced simulation and 1D projection techniques described in section 4.1 and so I delay discussion of this comparison until then.

3.5.3 Model weaknesses Although the high level of coarse-graining in the GO model has enabled the generation of useful results and a comparison with experimental data, the simplicity of the nucleus description also leads to some limitations. The high level of coarse-graining necessitates some modelling assumptions. In particular, *ad hoc* choices for the structure of the nucleus and the effective surface area for attachment of new stems were needed during the model's derivation. Ultimately, these choices will only be justified by comparison with more detailed simulation techniques.

The model also contains a number of quiescent crystallisation parameters.These parameters are τ_0, the basic monomer attachment timescale, ε_B, the bulk free energy gain upon crystallisation and μ_s, the interfacial free energy cost. Changes of these parameters with temperature will strongly influence the nucleation, yet the model has no mechanism to predict these changes. There may also be subtle changes with molecular weight, which the model also cannot predict. Again, results from more detailed simulations will help resolve these issues.

There are also some limitations of the flow modelling. Currently the GLaMM model[71] has been developed and validated for monodisperse and bidisperse molecular weight distributions. However, crystallisation experiments are almost always conducted on polydisperse materials. Consequently, when comparing to nucleation rate measurements, the polydisperse melt had to be approximated by a bimodal distribution, in order to capture the role of the high molecular weight tail. A further limitation is the GLaMM model's treatment of stretch fluctuations under flow. Real chains, subjected to non-linear

flow, are likely to show significant non-equilibrium fluctuations due to molecular individualism[77,78]. Experimental measures that characterise the flow of non-crystalline chains, such as mechanical stress[71] and neutron scattering[79] depend only on the mean chain deformation, which is computed by the GLaMM model. However, as nucleation is an intrinsically rare and discrete event that is strongly enhanced by highly stretched chains, it is likely that nucleation is disproportionately affected by rare non-equilibrium incursions into highly stretched states. In the GO model, stretch fluctuations are treated using an equilibrium technique. This is potentially underestimates the influence of flow. This final two limitations can be addressed within the framework of the GO model. However, they require improvements of the underlying rheological model on which the GO model relies.

4 Recent developments

In this section I summarise some recent developments in modelling polymer crystallisation. These recent studies build techniques that enable insight and quantitative results from one level of modelling to be exploited by modelling at a different level of coarse-graining.

4.1 The GO model

4.1.1 Fast nucleation algorithm The GO model algorithm is fast but still does not address the rare event problem. Nucleation barriers in experiments can typically be $\sim 80k_BT$ so nucleation in polymer experiments is extraordinarily rare. When simulating such high barriers, the overwhelming majority of the simulation time is spent resolving the dynamics of small nuclei that are close to the barrier base. As indicated by equation (2), these dynamics at the barrier base are irrelevant to the nucleation rate. Instead, it is the dynamics over the barrier peak that have the dominate contribution. However, in a direct nucleation simulation, these dynamics are sampled only vanishingly often and for an extremely short period.

My group recently developed a simulation technique to address this problem[80]. Our approach is inspired by the realisation that only the dynamics over the barrier peak are important and the suggestion from equation (2) that nucleation can be decomposed into two parts: injection of particles into the plateau region from an equilibrium distribution and diffusion across the plateau region. Our algorithm simulates the dynamics only over a reduced region, which is defined as $N_T > N_{min}$, where N_{min} is some minimum nucleus size. Our criterion for choosing N_{min} is described below.

We obtain the nucleation barrier through an equilibrium simulation. Here, reflecting boundary conditions are placed at both ends of the simulation. This simulation samples the equilibrium occupancy probability of each N_T value, from which the free energy can be obtained. As the barrier peak is very rarely visited, we constrain the simulation to a small region of the N_T space and piece together the whole barrier from a sequence of overlapping simulations. This ensures good sampling across all states, even for large nucleation barriers.

To simulate the dynamics over the plateau, nuclei are introduced at N_{min}, with their arrangement of monomers and stems drawn from the Boltzmann distribution. The nucleus dynamics are then simulated in the plateau region using the usual algorithm. Any run where N_T falls below N_{min} is restarted by reinserting the nucleus at N_{min}. We record the fraction of runs that successfully cross the barrier. The nucleation rate is then the product of the true flux into the plateau region and this success fraction. We compute the true flux into the plateau region as an average over the fluxes into N_{min} from the states immediately below, weighted by the Boltzmann distribution across the full barrier. The Boltzmann distribution is essentially exact for states with $N_T < N_{min}$, provided N_{min} is chosen such that $F(N_{min})$ is sufficiently smaller than F^*. In this case the resulting nucleation rate is independent of the choice of N_{min} and approximates very closely the nucleation rate from a direct simulation of the whole barrier. We found that $F^* - F(N_{min}) \approx 7k_BT$ is usually sufficiently large for accurate convergence with respect to N_{min}.

As the reduced simulation is always over a relatively modest barrier size our algorithm does not become more expensive with increasing barrier size. This enables essentially arbitrarily high barriers to be simulated inexpensively. Via this technique we were able to map out the model's predictions over a very wide range of input parameters[76]. This characterisation was key to validating or 1D projection method (see section 4.1.2) and to comparing the model to experimental data at a range of different temperatures (see section 4.1.3).

Our algorithm is related to the widely-applicable technique of milestoning[81], in which a rare event is simulated by linking together a sequence of simulations of sub-regions that cover the overall simulation space. However, a key difference of our method to milestoning is that only two sub-regions are considered, the barrier base and the barrier peak, and that the base of the barrier is not simulated, but is dealt with analytically.

4.1.2 1D projection method Projection of the polymer nucleation problem onto a low dimensional space is a key coarse-graining step. A low-dimensional projection groups together states in the high-dimensional simulation phase space, according to some property, for example the total nucleus size N_T. This new co-ordinate is intended to describe the progress toward nucleation using fewer degree of freedom (see fig 7). The projection converts a simulation algorithm into an analytically tractable problem, similar to classical nucleation theory, from which details of the nucleation process can be obtained as closed form expressions. This is a key step in pass-

ing insight from molecular simulations (which are intrinsically stochastic) to macroscale continuum models, for example by providing an analytic expression connecting the chain configuration under flow to the nucleation rate. In general these low dimensional projections are very difficult. One must identify a reaction co-ordinate and obtain both the barrier and diffusion rates for the dynamics projected onto this reaction co-ordinate.

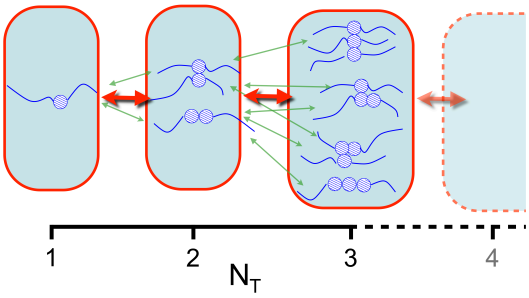

Fig. 7 A schematic illustration of our 1D projection approach. Here microscopic nucleus configurations containing the total number of monomers are collected together to form a lower dimensional co-ordinate for nucleation. The green arrows indicate microscopic moves whose rates must be averaged to produce diffusion rates along the new co-ordinate.

Locating appropriate reaction co-ordinates is a notoriously difficult problem[82]. However, to carry out such a projection for the GO model, we postulated a reasonable candidate reaction co-ordinate, namely the total nucleus size N_T, and demonstrated *a posteriori* that the resulting projection leads to a useful result[44]. To obtain the barrier, we use the same equilibrium technique as our fast nucleation algorithm (see section 4.1.1). We also require the diffusion rate between neighbouring states along the reaction co-ordinate, which will depend upon position along the co-ordinate. This diffusion rate is an average over the individual states that comprise a given value of N_T, weighted by the occupancy probabilities of the full barrier crossing problem. Thus analytic calculation of these diffusion rates is as intractable as solving the full high-dimensional barrier-crossing problem. Therefore, we developed a technique that reverse-engineers the problem by extracting the diffusion rates from our simulations. This ultimately leads to an analytical model that is extremely effective at predicting the nucleation rate for a very wide range of barriers, not just those used to characterise the projection.

Our 1D projection method is as follows[44]. For a discrete 1D system, detailed balance specifies that, in the uphill section of the barrier, the forward and reverse move rates from state i, k_i^+ and k_i^-, are given by

$$k_i^+ = D_i \exp(-(\Delta F_{i+1} - \Delta F_i)), \qquad k_{i+1}^- = D_i, \tag{3}$$

where ΔF_i is the 1D barrier, obtained above, and D_i is the collection of diffusion rates that we seek. For downhill sections of the barrier the expressions are similar, but the exponential term appears in the expression for k_{i+1}^-. In steady state the following net flux expression holds for each i

$$J = k_i^+ \chi_i - k_i^+ \chi_{i+1}, \tag{4}$$

where J is the total crossing rate and χ_i is the occupancy probability for the full non-equilibrium barrier crossing problem. Substituting eqn (3) into eqn (4) and rearranging gives an expression for D_i, in terms of quantities that can be extracted from our simulation of the full system

$$D_i = \frac{J}{\chi_i \exp(-(\Delta F_{i+1} - \Delta F_i)) - \chi_{i+1}}. \tag{5}$$

Thus for any given simulation we can always extract a 1D projection that has the same non-equilibrium occupancies, χ_i and overall crossing rate J as the full simulation. However, the projection algorithm is as numerically expensive as merely simulating the crossing rate. Therefore, the projection is only useful if it can predict the result of other simulations, for example with different barrier characteristics. This is the case with our projection of the GO model.

We performed the 1D projection for the GO model, employing a range of different quiescent barrier parameters (ΔF^* and n^*) and chain stretch ratios. We also simulated nucleation from bimodal blends, in which the short chains remained unstretched while long chains are allowed to stretch. We investigated a range long chain concentrations for these simulations[44]. In almost all cases, the results for D_i were virtually independent of the barrier characteristics and they fell on a mastercurve for D_i. This is a strong indication that our choice of reaction co-ordinate is appropriate and is leading us to diffusion measures that are indicative of some intrinsic underlying dynamics of the model. Furthermore, the master curve for D_i enables us to predict accurately the nucleation rate for virtually all parameter sets, through an analytical Kramers calculation (see section 3.1), without needing to run any further simulations. Finally, the form of D_i extracted from our simulations was very close to that obtained by assuming that all nuclei remain spherical throughout nucleation.

There are some deviations from the spherical behaviour in the kinetics extracted from our GO model simulations, for bimodal blends. These deviations are most pronounced for dilute long chains, subjected to high stretch. Such conditions lead to highly elongated nucleation in the GO model. This suggests that when elongated nucleation occurs, our choice of 1D reaction co-ordinate becomes inappropriate and, probably, a more detailed co-ordinate with two or more dimensions is required to systematically describe this region of the model.

With a 1D model for the nucleus diffusion kinetics in hand, we now seek a method to analytically obtain the 1D nucleation barrier for stretched chains. Although a full analytical solution

to this problem is possible[83] the resulting expressions are sufficient unwieldy to be unusable in practise. Instead we simulated nucleation barriers for a wide range of quiescent barriers and degrees of chain stretching[76]. These results show that, for monodisperse polymers, the chain deformation modifies the quiescent barrier with a term this is a simple function of the chain stretching alone, independent of the quiescent barrier. Hence the 1D landscape under flow can readily be calculated for monodisperse chains. Unfortunately, the barrier modification for bimodal blends is a nonlinear function of ΔF^*, n^* and the degree of stretch. Therefore we developed a semi-analytical method to rescale a small set of reference data for the flow-induced barriers to predict barriers for any model parameters. This rescaling method enables us to compute the nucleation rate for the GO model for any reasonable combination of ΔF^*, n^*, chain stretch and long chain concentration.

4.1.3 Comparison with experiments We recently performed[76] a quantitative comparison of the GO model with direct nucleation rate measurements from a flowing melt by Pantani and coworkers[17,18]. These measurements were made on a polydisperse isotactic polypropylene (iPP) melt in steady shear, at a range of shear rates and temperatures. To model these data with the GO model, we approximated this fully polydisperse material as a bimodal blend[69]. There is no single obvious position to define the division between the high and low molecular weight fractions of the melt and so we took the final 1% of the molecular weight distribution as the long chain component. Flow parameters could be accurately determined from literature values and were confirmed against linear rheological measurements[69]. However, the crystallisation parameters could only be estimated from the literature and final values were determined by fitting to the flow-induced nucleation data. In order to predict the nucleation rate we require the basic move attempt timescale τ_0 and the quiescent values of ΔF^* and n^* (or equivalently, the bulk and interfacial free energy parameters ε_b and μ_s). The basic move rate τ_0 could be estimated from the monomer diffusion time that is implied by the rheological relaxation times, ΔF^* can be estimated by considering the ratio of the quiescent nucleation rate to τ_0 and n^* can be estimated by assuming the critical nucleus size to be of the same order as the lamella thickness[84]. We obtained the final values of these crystallisation parameters by fitting to the iPP nucleation rate data[17], across the full range of measured flow rates, at 140°C. Essential to this fitting process was the 1D projection method described in section 4.1.2, which enabled rapid evaluation of the GO model's nucleation rate predictions as a function of the input parameters, without the need for numerically expensive simulations.

Having fitted the values for a single temperature (140°C) we extended the comparison to the two additional experimental temperatures[18]. We assumed that μ_S does not change significantly with temperature and that τ_0 shifts in the same way as the rheological timescales. This leaves the bulk free energy of crystallisation ε_B as the only free parameter for each of the two new temperatures. The result of fitting ε_B is shown in fig 8. The model captures well the experimental data, confirming that changes in entropy upon stretching are sufficient to account for observed enhancement of nucleation. There is some systematic disagreement at the highest shear rate for each temperature. At these highest shear rates, the model overpredicts the nucleation rate, suggesting that some addition factor suppresses the acceleration of shear-induced nucleation. It may be that, at high shear rates, the finite supply of long chains begins to locally exhaust as nuclei are formed.

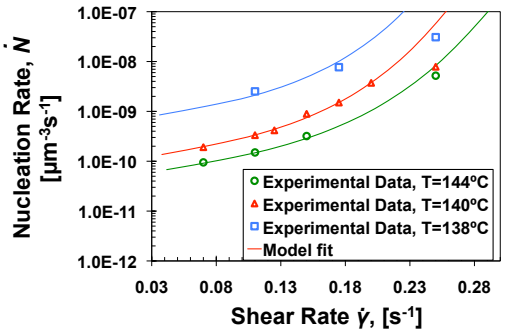

Fig. 8 Comparison of the GO model's nucleation rate predictions to experimental measurements of the nucleation rate from an iPP melt undergoing steady shear at several temperatures[17,18].

The experimental nucleation rate data in fig 8 show an increased sensitivity to shear as the temperature increases. That is, the general slope of the nucleation rate with shear rate increases with temperature. The GO model successfully predicts this trend and provides a molecular explanation. As the temperature increases so does the quiescent critical nucleus size, n^*, due to the weaker thermodynamic driving force for crystallisation. For larger n^* a greater number of stretched segments can be incorporated into the nucleus before it grows beyond the critical size, giving a correspondingly larger reduction in the nucleation barrier due to chain stretching.

4.2 Molecular dynamics

Yi *et al.*[56,57,85] have recently performed an intriguing series of molecular dynamics simulations. Although these simulations concern only quiescent nucleation, they highlight potential pathways to progress in FIC. The simulations contain two key innovations that involve the interplay of very detailed MD simulations with the analytic modelling of classical nucleation theory. Firstly, they used MD simulations to extract both the interfacial energies for classical nucleation theory and details of the nucleus topology along the nucleation pathway. Sec-

ondly, they used concepts from classical nucleation theory to extend their results to lower undercooling where the nucleation rate is not accessible by direct simulation. This provides the a quantitative model of homogeneous nucleation in polymers derived from first principles, along with a methodology by which MD simulations can inform the modelling assumptions required for more tractable approaches.

Yi *et al.* performed direct MD simulations of nucleation of polyethylene chains at about 30% undercooling. From these data, they used first passage time analysis to extract the nucleation rate and identify the critical nucleus size n^*. They studied chains with 8, 20, 150 and 1000 carbons[56,57,85], with the latter two chains being long enough to exhibit chain folding when crystallised. Monte-Carlo sampling of the free energy barrier, also confirmed the barrier properties obtained by first passage time analysis[85]. A cylindrical model, based on classical nucleation theory, was used to characterise the nucleus shape and to extract the interfacial free energies. The nucleation rates obtained for the longest two chains were almost identical. This indicates that nucleation, at this high undercooling, is controlled by the local environment, which is insensitive to molecular weight. Indeed, even nuclei of ~ 800 atoms involved only short segments the chains.

Using the survival probability method, the critical nucleus size was determined as a function of temperature. This avoids the need for direct simulations at higher temperature as the nucleation pathways obtained for 30% undercooling were assumed to be valid at high temperatures. This approach provides n^* as a function of temperature, along with the variation of the two interfacial free energies. For the longest chains, the interfacial free energies were found to vary strongly with temperature. These interfacial free energies were then combined with the Gibbs free energy difference between the crystal and melt phases, which was calculated from the degree of undercooling, to compute the nucleation barrier. The computed free energy barrier and the segmental dynamics, were then used in a classical nucleation calculation, which lead to the temperature dependence of the nucleation rate.

5 Open questions and future directions

5.1 Future directions

There is still significant new research that is required in order to meet the ultimate goal of multiscale modelling in polymer crystallisation: that is, to drive insight and quantitative results gained from the most detailed level of simulations, through the various coarse-graining levels, to derive macroscale continuum models that simultaneously have deep-rooted molecular origins and yet are suitable to model polymer processing.

I have described here a few examples of this methodology in practice. These include work by Rutledge and coworkers[56,57,85] and Howard and Milner[51,52] to extract the parameters for classical nucleation theory from detailed molecular simulations. Another example is my group's work to project the GO model onto an analytically tractable low dimensional model[44]. Such approaches, that unite models across different levels of coarse-graining, are needed at all modelling levels in fig 3. This will require insight, new techniques and the adoption of ideas from other areas[86]. A key factor will be identifying which quantities to extract from detailed simulations to resolve the coarse-graining assumptions in less detailed techniques and to produce the closest correspondence between neighbouring models.

A significant issue with stochastic simulation of nucleation is the rare event problem. Specifically, although successful nucleation events will be relatively fast, they occur so rarely that the simulation times required to directly observe nucleation are too long. These fluctuation-driven rare events are ubiquitous in molecular science, for example in chemical reactions, branched polymer dynamics and protein folding. Hence there already exists a wide range of techniques to simulate rare events. Some methods rely on an *a priori* specification of an order parameter. The maximum of the free energy along this order parameter must capture well the dynamically important states that are at the cusp between progressing or failing (i.e. the transition state). These approaches include Chandler's method[87,88] and milestoning[81]. Intrinsic to these methods is an insightful choice of order parameter. There are also alternative methods where the order parameter does not impose assumptions on the pathways and only distinguishes between the initial and final states, such as Transition Path Sampling[82], which has been generalised to non-equilibrium[89] and to non-stationary[90] systems. I have discussed above how such techniques have been used to solve the rare event problem in simulations of the GO model[80]. A key step will be identifying which techniques are suitable for MD and lattice MC simulations of polymer nucleation under flow.

The 1D projection algorithm, described in section 4.1.2, effectively produced an analytic expression for the nucleation rate in the GO model. This enabled an effective comparison with experimental data and provides key results towards deriving a macroscale continuum model from the GO simulation algorithm. An important next step will be extending this method to capture high shear rates, where oriented and elongated nuclei develop. It seems likely that a higher dimensional projection will be required to account for the higher number of degrees of freedom (e.g. nucleus size, aspect ratio and long chain composition) that are needed to describe these shish-like nuclei. Another key step will be to apply this methodology to MD and lattice MC simulations. The greater spatial resolution of these simulations will test whether the total nucleus size is a suitable projection for these more detailed simulations. Moreover, the diffusion constants extracted by technique will give

a clear measure of the effective surface area available for attachment in a polymer nucleus.

Every level of modelling requires a method to impose flow onto the nucleation simulation. Although there are established methods for molecular dynamics[53,62,91], other levels of coarse-graining require new approaches. For example, Hu *et al.*(2002)[40] used a single aligned chain to mimic the effect of flow on long chains. However, this approach cannot be directly related to any particular flow rate or geometry. The GO model relies on a rheological model to predict the amorphous chain deformation under flow. It currently uses a model that has been validated for both monodisperse[71] and bimodal[72] molecular weight distributions. Macroscale continuum models similarly rely on rheological models. Further development of molecular flow models is needed as there is currently no widely validated model for non-linear flow of polydisperse polymers. Validating such a model for use in FIC modelling is likely to require more than just comparison to mechanical stress measurements. This is because very long chains at a concentration of a few percent or less affect the bulk stress only under very specific flow conditions. In contrast, it is known that highly stretched chains at concentrations as low as 0.5% still dominate flow-induced nucleation[11]. Recent neutron scattering measurements on flowing bimodal blends have isolated the contribution from the long chain fraction[72] and this is a promising technique for determining the high molecular weight tail dynamics in polydisperse polymers.

5.2 Open questions.

Despite the progress described above, there remain a number of unsolved modelling problems in polymer nucleation. Some relate to physical questions about the underlying nucleation mechanism, while others concern the approaches required to enable fully integrated multiscale modelling.

What is the shish kebab formation mechanism? Experimental evidence suggests that shish formation is a multistage process[26–28], which may require cooperation between multiple densely packed precursors. This poses a number of questions. What is the nature of the order in the shish precursor? How does this precursor promote shish nucleation? What role does flow-induced liquid-liquid separation play? Are these structures formed from isolated elongated structures as in the GO model or, instead, through the aggregation of trains of closely packed precursors that are more spherically shaped? Understanding these mechanisms will be essential to controlling and optimising the favourable properties that shish-kebabs imbue to solidified materials.

How does polydispersity affect the nucleation barrier? It is clear that the concentration of stretched chains influences both the nucleation rate and the crystal morphology. The GO model accounts for bimodal blends, and can be generalised to polydisperse systems. However, there is currently no reliable way to predict the effect of concentration on the nucleation barrier even for the simplest polydisperse system, bimodal blends. However, experiments and polymer processing invariably involve fully polydisperse systems. A reliable method to compute the nucleation barrier for an arbitrary mixture of chains of varying degrees of stretch is one method to obtain an analytic model. Furthermore, the more detailed simulation techniques, such as MD and lattice MC, have yet to explore polydisperse systems, perhaps because of the large simulation box sizes that are required to accommodate long chains and to ensure good sampling of the most rarely occurring chains.

What is the correct low-dimensional projection for polymer nucleation? Projecting molecular simulations onto lower dimensional models is a key step in producing tractable models that are free of stochastic terms. Essential to this projection is an effective choice of the reaction co-ordinate. A reaction co-ordinate is a low-dimensional path through the system's phase space that provides a good measure of the progression towards nucleation. More specifically, a "good" reaction co-ordinate will be a strong predictor of the whether the trajectory is fated to progress to the final state or to return to the initial state. However, reaction co-ordinates are notoriously difficult to determine even for well-studied systems, because the dynamically relevant pathways are a complicated function of the system's interactions and dynamics. A commonly used quantity in discussing reaction co-ordinates is the committor probability[92]. This is the fraction of trajectories that successfully reach the final state, when released from a given point. The optimal reaction co-ordinate is normal to the surface of equal committor probabilities[93]. Unfortunately, isocommittor surfaces are extremely expensive to compute.

Despite these difficulties, some useful results have been derived using *ad hoc* reaction co-ordinates, i.e. projections that have not been demonstrated to comply fully with the requirement of a reaction co-ordinate. For example, Hamer *et al.*[44] used the total nucleus size N_T and a number of studies[51,57,63] have used the cylindrical nucleus model. The useful results gained from these works suggests that, although these intuitively chosen co-ordinates are not fully orthogonal to the isocommittor surfaces, they still provide a serviceable measure of the extend of nucleation. This is, perhaps, because the most dynamically relevant pathways to nucleation are sufficiently narrow that the reaction co-ordinate need only be approximately orthogonal to the isocommittor surface in a small region around the most likely nucleation path. Indeed Yi *et al.*[57] demonstrated that different choices for the reaction co-ordinate give slightly different barriers but the same overall crossing rate. However, detailed studies on crystal nucleation in Lennard-Jones fluids[94], have shown that nucleation occurs along many distinct pathways, encompassing both well-ordered compact nuclei and large, less ordered nuclei, imply-

ing that the reaction co-ordinate must include both the cluster size and the quality of the crystal structure.

From the work of Hamer *et al*[44], it also seems possible that the dimensionality of the projection may have to change with flow rate, to account for the transition from point-like to thread-like nuclei. As the shish kebab formation mechanism remains unclear it is also unknown whether a projection is even suitable in this case. Further work is needed to give less ambiguous and *ad hoc* answers to these questions and to provide a more systematic framework[86] for selecting reaction co-ordinates for polymer nucleation, particularly under flow.

Which simulation techniques for rare events can be applied to polymer nucleation? A key problem for modelling nucleation in polymers is the difficulty in simulating rare events. This issue affects all levels of coarse-graining that require stochastic simulation. As rare events are ubiquitous in molecular science, a range of simulation techniques have been developed to address this general problem, as discussed in section 5.1. These techniques have been shown, in other contexts, to be extremely effective. An important future task will be to apply and adapt these algorithms to nucleation in polymers.

Some work addressing the difficulties of direct simulation of nucleation has been carried out. My group recently applied a method similar to milestoning to solve the rare event problem in the GO model[80]. Furthermore, Yi *et al.* used a survival probability method to obtain nucleation rates, via classical nucleation theory. Yi *et al.*'s method relies upon nucleation paths that are obtained from direct simulation at high undercooling remaining valid at higher temperatures. This is essentially the assumption that the reaction co-ordinate does not change appreciably with temperature. At very low undercooling or under strong flow the appropriate reaction co-ordinate is likely to change due to qualitative changes in the nucleation mechanism. Their method also relies on classical nucleation theory holding in the region of interest. Both assumptions may well be justified over a range of temperatures and perhaps even under flow. However, the reliability of this potentially very useful coarse-graining technique should ideally be verified against separate simulations, either by direct simulation or using an alternative fast nucleation algorithm.

How to incorporate flow into fast nucleation algorithms? Even though flow hugely enhances the nucleation rate, fast nucleation algorithms will still be required to simulate low undercooling. In principle this is extremely problematic as the dynamics under flow are non-reversible, which rules out many of the rare event algorithms. There are exceptions to this, such as forward flux sampling[89], which provide one possible avenue for progress. A further possibility is offered by the quasi-static result that was found for the GO model[69]. This suggests that the separation of timescale between the slow flow dynamics and rapid local crystallisation dynamics means that chains can be held fixed in their instantaneous flow-induced configuration in order to sample the resulting instantaneous nucleation rate. This approximation would allow the use of rare event algorithms that rely on reversible dynamics. Within in the GO model freezing the chain configurations is straightforward as the chain stretching under flow and nucleation dynamics are modelled by separate algorithms. However, in molecular dynamics simulations the flow is imposed on the simulation box. Thus, to exploiting the quasi-static result requires some method hold the chains fixed in their flow-induced configurations during the fast nucleation simulation. There is no unambiguously correct way to implement this, however, it may be possible to exploit the separation of lengthscales between the flow dynamics and the nucleation dynamics to locate a lengthscale above which the chains should be held fixed. Some experimentation with different algorithms, combined with comparison with direct nucleation simulations, where possible, will be need to establish a reliable approach.

What is the role of the specific work? In particular, it is not established why the macroscopically imposed specific work summarises so well experimental data that encompasses variations in flow rate and flow time. Furthermore, it is not understood why the specific work appears to control both the nucleation density and the threshold for shish-kebabs. Nevertheless, these are well-supported empirical facts, which currently have no theoretical explanation. Although the specific work is fundamentally a macroscopic quantity, it should be relatable to some molecular quantity. Ideally, the specific work should emerge as a prediction of a molecular argument that can predict the variation of the critical work with chemistry and molecular weight distribution, rather than being an input assumption[3]. As the specific work summarises large amounts of experimental observation, understanding its origin will be of great use to the development of continuum level models.

How does the crystal morphology influence the solid state properties? It is known that the crystal morphology hugely influences solid state properties. For example, shish-kebabs improve mechanical properties[20] and reduce permeability[21]. However, in order to optimise final product properties a quantitative understanding of the connection between morphology and solid properties is required. A key factor is the number of tie molecules and chain entanglements[95]. Both structures involve topologically constrained links between separate lamella caused by amorphous sections of chain. These links significantly improve mechanical properties, particularly crack resistance. Information on these formations is accessible from detailed simulations and must be included in more coarse-grained approaches.

6 Conclusions

Flow induced nucleation in polymers is significant to both fundamental science and practical industrial processing. A

detailed molecular understanding of flow-induced nucleation would enable polymer processors to tailor and optimise the solid state properties of polymer products by controlling processing conditions. The most pronounced flow-induced affects occur for long chains and at low undercooling. Understanding this regime is essential, but it presents the most formidable modelling issues.

Polymer crystallisation involves a huge spread of both length and timescale: the dynamics emerge from local monomer motion but crystallisation leads to structures the size of whole chains, or bigger, that develop on macroscopically slow timescales. Multiscale modelling is essential to bridge gaps in both length and timescales. There are a wide range of simulation techniques that are applicable to polymer nucleation, from molecular dynamics to highly coarse-grained kinetic Monte-Carlo approaches. Tight integration of the various levels of simulation is essential to ensure that more tractable approaches retain the correct molecular physics.

There is a further timescale problem that arises because nucleation is a rare event: the system makes frequent attempts to nucleate but fails in the overwhelming majority of cases. The success fraction decreases exponentially with the height of the nucleation barrier and becomes extremely small at lower undercooling. Therefore direct simulation requires very small timesteps but must access very long timescales to observe a statistically significant number of nucleation events. As this difficulty affects all levels of modelling that rely on stochastic simulation, it cannot be solved by coarse-grained algorithms alone. However, there are simulation approaches that address the issue of rare events. Recent attempts to apply some of these ideas to polymer nucleation have begun to extend the range of temperature that can be simulated. Many more sophisticated approaches to rare event simulation have been developed from the numerous fields that are afflicted by this common difficulty. A key next step will be applying and adapting these techniques for polymer nucleation. Particular care will be required to produce techniques that remain rigorous even in the presence of strong flow.

Finally, the full potential of modelling polymer FIC will only be achieved if molecular insight can be translated into quantitative modelling of polymer processing, ultimately leading to optimisation of polymer products. This demands tractable models that are free of stochastic terms. One method to derive these macroscale continuum models is to project expensive simulations onto a lower dimensional model, which can then be solved analytically using techniques from classical nucleation theory. This approach is fraught with the difficult of identifying an appropriate reaction co-ordinate. Some recent approaches have made successful progress using intuitively estimated co-ordinates. Future progress will depend upon a deeper understanding of which co-ordinate choices are acceptable, leading towards a more systematic approach to obtaining co-ordinates and establishing their reliability.

Acknowledgements

I thank Matthew Hamer, Kenny Jolley, Peter Olmsted, Daniel Read and Gerrit Peters for numerous interesting and stimulating discussions. I thank Profs Alexei Likhtman and Wenbing Hu for providing images used in fig 3. I gratefully acknowledge funding from the EPSRC (grant no. EP/G048827/1) and access to the University of Nottingham High Performance Computing Facility.

References

1 F. L. Binsbergen, *Nature*, 1966, **211**, 516–517.
2 A. Keller and H. Kolnaar, *Processing of Polymers*, Wiley-VCH, Weinheim, 1997, vol. 18, p. 189.
3 L. Scelsi, M. R. Mackley, H. Klein, P. D. Olmsted, R. S. Graham, O. G. Harlen and T. C. B. McLeish, *J Rheol*, 2009, **53**, 859–876.
4 R. S. Graham, *J Eng Math*, 2011, **71**, 237–251.
5 S. Kimata, T. Sakurai, Y. Nozue, T. Kasahara, N. Yamaguchi, T. Karino, M. Shibayama and J. A. Kornfield, *Science*, 2007, **316**, 1014–1017.
6 O. O. Mykhaylyk, P. Chambon, R. S. Graham, J. P. A. Fairclough, P. D. Olmsted and A. J. Ryan, *Macromolecules*, 2008, **41**, 1901–1904.
7 T. Kanaya, I. A. Polec, T. Fujiwara, R. Inoue, K. Nishida, T. Matsuura, H. Ogawa and N. Ohta, *Macromolecules*, 2013, **46**, 3031–3036.
8 M. Doi and S. F. Edwards, *The Theory of Polymer Dynamics*, Oxford University Press, Oxford, 1986.
9 E. L. Heeley, C. M. Fernyhough, R. S. Graham, P. D. Olmsted, N. J. Inkson, J. Embery, D. J. Groves, T. C. B. McLeish, A. C. Morgovan, F. Meneau, W. Bras and A. J. Ryan, *Macromolecules*, 2006, **39**, 5058–5071.
10 G. Kumaraswamy, A. M. Issaian and J. A. Kornfield, *Macromolecules*, 1999, **32**, 7537–7547.
11 M. Seki, D. W. Thurman, J. P. Oberhauser and J. A. Kornfield, *Macromolecules*, 2002, **35**, 2583–2594.
12 S. Coppola, L. Balzano, E. Gioffredi, P. L. Maffettone and N. Grizzuti, *Polymer*, 2004, **45**, 3249–3256.
13 E. E. Bischoff-White, H. H. Winter and J. P. Rothstein, *Rheologica Acta*, 2012, **51**, 303–314.
14 A. Godara, D. Raabe, P. van Puyvelde and P. Moldenaers, *Polymer Testing*, 2006, **25**, 460–469.
15 G. Eder and H. Janeschitz-Kriegl, *Processing of Polymers*, Wiley-VCH, Weinheim, 1997, vol. 18, p. 269.
16 M. Stadlbauer, H. Janeschitz-Kriegl, G. Eder and E. Ratajski, *J. Rheol.*, 2004, **48**, 631–639.
17 I. Coccorullo, R. Pantani and G. Titomanlio, *Macromolecules*, 2008, **41**, 9214–9223.
18 R. Pantani, I. Coccorullo, V. Volpe and G. Titomanlio, *Macromolecules*, 2010, **43**, 9030–9038.
19 B. S. Hsiao, L. Yang, R. H. Somani, C. A. Avila-Orta and L. Zhu, *Phys. Rev. Lett.*, 2005, **94**, 117802.
20 Z. Bashir, J. A. Odell and A. Keller, *J Mater Sci*, 1986, **21**, 3993–4002.
21 *Handbook of Polyolefins*, ed. C. Vasile, Dekker, New York, 2000.
22 N. Tian, W. Zhou, K. Cui, Y. Liu, Y. Fang, X. Wang, L. Liu and L. Li, *Macromolecules*, 2011, **44**, 7704–7712.
23 D. Liu, N. Tian, K. Cui, W. Zhou, X. Li and L. Li, *Macromolecules*, 2013, **46**, 3435–3443.

24 K. Cui, L. Meng, Y. Ji, J. Li, S. Zhu, X. Li, N. Tian, D. Liu and L. Li, *Macromolecules*, 2014, **47**, 677686.
25 L. Balzano, *PhD thesis*, Eindhoven University of Technology, 2008.
26 L. Balzano, N. Kukalyekar, S. Rastogi, G. W. M. Peters and J. C. Chadwick, *Phys. Rev. Lett.*, 2008, **100**, 048302.
27 L. Balzano, S. Rastogi and G. Peters, *Macromolecules*, 2011, **44**, 2926–2933.
28 L. Balzano, S. Rastogi and G. W. M. Peters, *Macromolecules*, 2009, **42**, 2088–2092.
29 F. Azzurri and G. C. Alfonso, *Macromolecules*, 2005, **38**, 1723–1728.
30 F. Azzurri and G. C. Alfonso, *Macromolecules*, 2008, **41**, 1377–1383.
31 D. Cavallo, F. Azzurri, L. Balzano, S. S. Funari and G. C. Alfonso, *Macromolecules*, 2010, **43**, 9394–9400.
32 Y. Hayashi, G. Matsuba, Y. Zhao, K. Nishida and T. Kanaya, *Polymer*, 2009, **50**, 2095–2103.
33 Y. Zhao, G. Matsuba, K. Nishida, T. Fujiwara, R. Inoue, I. Polec, C. Deng and T. Kanaya, *J. Polym. Sci. B Polym. Phys.*, 2010, **49**, 214–221.
34 C. Deng, T. Fujiwara, I. Polec, G. Matsuba, L. Jin, R. Inoue, K. Nishida and T. Kanaya, *Macromolecules*, 2012, **45**, 4630–4637.
35 I. A. Polec, T. Fujiwara, T. Kanaya and C. Deng, *Polymer*, 2012, **53**, 3540–3547.
36 T. Hashimoto, H. Murase and Y. Ohta, *Macromolecules*, 2010, **43**, 6542–6548.
37 H. Murase, Y. Ohta and T. Hashimoto, *Macromolecules*, 2011, **44**, 7335–7350.
38 O. O. Mykhaylyk, C. M. Fernyhough, M. Okura, J. P. A. Fairclough, A. J. Ryan and R. Graham, *European Polymer Journal*, 2011, **47**, 447–464.
39 M. Okura, O. O. Mykhaylyk and A. J. Ryan, *Phys Rev Lett*, 2013, **110**, 087801.
40 W. Hu, D. Frenkel and V. Mathot, *Macromolecules*, 2002, **35**, 7172–7174.
41 H. A. Kramers, *Physica*, 1940, **VII**, 284–304.
42 D. Turnbull and J. C. Fisher, *Journal Of Chemical Physics*, 1949, **17**, 71–73.
43 G. Strobl, *Rev. Mod. Phys.*, 2009, **81**, 1287–1300.
44 M. J. Hamer, J. A. D. Wattis and R. S. Graham, *Soft Matter*, 2012, **8**, 11396–11408.
45 H. Janeschitz-Kriegl, *Progress in Colloid and Polymer Science*, 1992, **87**, 116.
46 W. Schneider, A. Köppl and J. Berger, *Int. Polym. Proc. II*, 1988, **3**, 151.
47 F. J. M. F. Custódio, R. J. A. Steenbakkers, P. D. Anderson, G. W. M. Peters and H. E. H. Meijer, *Macromol. Theory Simul.*, 2009, **18**, 469–494.
48 H. Zuidema, G. W. M. Peters and H. E. H. Meijer, *Macromol. Theor. Simul.*, 2001, **10**, 447–460.
49 S. Coppola, N. Grizzuti and P. L. Maffettone, *Macromolecules*, 2001, **34**, 5030–5036.
50 R. J. A. Steenbakkers and G. W. M. Peters, *J Rheol*, 2011, **55**, 401–433.
51 M. P. Howard and S. T. Milner, *Macromolecules*, 2013, **46**, 6593–6599.
52 M. P. Howard and S. T. Milner, *Macromolecules*, 2013, **46**, 6600–6612.
53 M. J. Ko, N. Waheed, M. S. Lavine and G. C. Rutledge, *J. Chem. Phys.*, 2004, **121**, 2823–2832.
54 R. Gee, N. Lacevic and L. Fried, *Nat Mater*, 2006, **5**, 39–43.
55 T. Yamamoto, *J Chem Phys*, 2010, **133**, 034904.
56 P. Yi and G. C. Rutledge, *J. Chem. Phys.*, 2009, **131**, 134902.
57 P. Yi, C. R. Locker and G. C. Rutledge, *Macromolecules*, 2013, **46**, 4723–4733.
58 N. A. Romanos and D. N. Theodorou, *Macromolecules*, 2010, **43**, 5455–5469.
59 T. Yamamoto, *Polymer*, 2009, **50**, 1975–1985.
60 N. Waheed, M. J. Ko and G. C. Rutledge, *Polymer*, 2005, **46**, 8689–8702.
61 T. Yamamoto, *Polymer*, 2004, **45**, 1357–1364.
62 M. S. Lavine, N. Waheed and G. C. Rutledge, *Polymer*, 2003, **44**, 1771–1779.
63 W. Hu, D. Frenkel and V. B. F. Mathot, *Macromolecules*, 2003, **36**, 8178–8183.
64 W. Hu and D. Frenkel, *Adv. Polym. Sci.*, 2005, **191**, 1–35.
65 G. Xu, H. Lin and W. L. Mattice, *J. Chem. Phys.*, 2003, **119**, 6736.
66 D. Frenkel and B. Smit, *Understanding Molecular Simulation: From Algorithms to Applications*, Academic Press, New York, 2002.
67 Y. Nie, H. Gao, M. Yu, Z. Hu, G. Reiter and W. Hu, *Polymer*, 2013, **54**, 3402–3407.
68 Y. Nie, H. Gao, Y. Wu and W. Hu, *Soft Matter*, 2014, **10**, 343.
69 R. S. Graham and P. D. Olmsted, *Phys Rev Lett*, 2009, **103**, 115702.
70 R. S. Graham and P. D. Olmsted, *Faraday Discuss*, 2010, **144**, 71–92.
71 R. S. Graham, A. E. Likhtman, T. C. B. McLeish and S. T. Milner, *J. Rheol.*, 2003, **47**, 1171–1200.
72 R. S. Graham, J. Bent, N. Clarke, L. R. Hutchings, R. W. Richards, T. Gough, D. M. Hoyle, O. G. Harlen, I. Grillo, D. Auhl and T. C. B. McLeish, *Soft Matter*, 2009, **5**, 2383–2389.
73 D. T. Gillespie, *J Phys Chem*, 1977, **81**, 2340–2361.
74 D. Sadler and G. Gilmer, *Phys Rev Lett*, 1986, **56**, 2708–2711.
75 J. Doye and D. Frenkel, *Phys Rev Lett*, 1998, **81**, 2160–2163.
76 K. Jolley and R. S. Graham, *Rheologica Acta*, 2013, **52**, 271–286.
77 P. G. De-Gennes, *Science*, 1997, **276**, 1999–2000.
78 R. E. Teixeira, A. K. Dambal, D. H. Richter, E. S. G. Shaqfeh and S. Chu, *Macromolecules*, 2007, **40**, 2461–2476.
79 J. Bent, L. R. Hutchings, R. W. Richards, T. Gough, R. Spares, P. D. Coates, I. Grillo, O. G. Harlen, D. J. Read, R. S. Graham, A. E. Likhtman, D. J. Groves, T. M. Nicholson and T. C. B. McLeish, *Science*, 2003, **301**, 1691–1695.
80 K. Jolley and R. S. Graham, *J Chem Phys*, 2011, **134**, 164901.
81 A. Faradjian and R. Elber, *J Chem Phys*, 2004, **120**, 10880–10889.
82 P. G. Bolhuis, D. Chandler, C. Dellago and P. L. Geissler, *Annu. Rev. Phys. Chem.*, 2002, **53**, 291–318.
83 M. J. Hamer, J. A. D. Wattis and R. S. Graham, *J Non-Newton Fluid Mech*, 2010, **165**, 1294–1301.
84 R. Olley and D. Bassett, *Polymer*, 1989, **30**, 399–409.
85 P. Yi and G. C. Rutledge, *J. Chem. Phys.*, 2011, **135**, 024903.
86 A. Ferguson, A. Panagiotopoulos, I. Kevrekidis and P. Debenedetti, *Chemical Physics Letters*, 2011, **509**, 1–11.
87 D. Chandler, *J Chem Phys*, 1978, **68**, 2959–2970.
88 S. Auer and D. Frenkel, *Adv Polym Sci*, 2005, **173**, 149–208.
89 R. J. Allen, C. Valeriani and P. R. ten Wolde, *J Phys-Condens Mat*, 2009, **21**, 463102.
90 N. B. Becker, R. J. Allen and P. R. ten Wolde, *J. Chem. Phys.*, 2012, **136**, 174118.
91 A. W. Lees and S. F. Edwards, *J. Phys. C: Solid State Phys.*, 2001, **5**, 1921–1928.
92 L. Onsager, *Phys. Rev.*, 1938, **54**, 554–557.
93 A. Berezhkovskii and A. Szabo, *J. Chem. Phys.*, 2005, **122**, 014503.
94 D. Moroni, P. T. Wolde and P. Bolhuis, *Phys Rev Lett*, 2005, **94**, 235703.
95 R. Seguela, *J. Polym. Sci. B Polym. Phys.*, 2005, **43**, 1729–1748.